

# Proposing optimum parameters of TMDs using GSA and PSO algorithms for drift reduction and uniformity

Nadia M. Mirzai<sup>1a</sup>, Seyed Mehdi Zahrai<sup>\*2</sup> and Fatemeh Bozorgi<sup>3b</sup>

<sup>1</sup>School of Civil Engineering, College of Engineering, the University of Tehran, Tehran, Iran

<sup>2</sup>Center of Excellence for Engineering and Management of Civil Infrastructures, School of Civil Engineering, College of Engineering, the University of Tehran, Tehran, Iran

<sup>3</sup>School of Civil Engineering, Iran University of Science and Technology, Tehran, Iran

(Received July 17, 2016, Revised June 5, 2017, Accepted June 6, 2017)

**Abstract.** In this study, the optimum parameters of Tuned Mass Dampers (TMDs) are proposed using Gravity Search Algorithm (GSA) and Particle Swarm Optimization (PSO) to reduce the responses of the structures. A MATLAB program is developed to apply the new approach to the benchmark 10 and 40-story structures. The obtained results are compared to those of other optimization methods used in the literature to verify the developed code. To show the efficiency and accuracy of the proposed methods, nine far-field and near-field worldwide earthquakes are applied to the structures. The results reveal that in the 40-story structure, GSA algorithm can reduce the Relative Displacement (RD) and Absolute Acceleration (AA) up to 43% and 21%, respectively while the PSO decreases them by 50% and 25%, respectively. In contrast, both GSA and PSO algorithms reduce the RD and AA about 29% and 21% for the 10-story structure. Furthermore, using the proposed approach the required TMD parameters reduce by 47% and 63% in the 40 and 10-story buildings in comparison with the referenced ones. Result evaluation and related comparison indicate that these methods are more effective even by using smaller TMD parameters resulting in the reduction of acting force from TMD, having smaller stiffness and damping factors while being more cost effective due to its decreased parameters. In other words, the TMD with optimum parameters can play a positive role in both tall and typical structures.

**Keywords:** GSA algorithm; PSO algorithm; TMD; optimization; vibration reduction

## 1. Introduction

Buildings with passive, active and semi-active control devices have been studied during the past decades. The Tuned Mass Damper (TMD) is one of the simplest control devices among the several passive control methods. Despite the progress of active and semi-active control systems in structural engineering, the passive control systems are still in use in many tall buildings due to their simplicity and lower cost. These passive systems use mechanical devices to dissipate a part of the input energy. Therefore, the structural responses and damages reduce too.

The primary form of TMD has been used by Frahm (1911). This device was useful only when the frequency of the input excitation was so close to the natural frequency of the device. Later in 1947, optimal parameters of TMD were discussed by Ormondroyd and Den Hartog. At first, this theory was only appropriate for an undamped SDOF system under a sinusoidal force excitation. The theory was extended to damped SDOF systems by many researchers

(Warburton and Ayorinde 1980, Randall *et al.* 1981, Warburton 1982, Tsai and Lin 1993). Thompson (1981) also used the frequency method for optimizing TMD parameters. The genetic algorithm has been widely used in tuning TMDs as well (Hadi and Arfiadi 1998, Singh *et al.* 2002, Desu *et al.* 2006, Pourzeynali *et al.* 2007). Lee *et al.* (2006) improved Shuffled Complex Evolution (SCE) algorithm to reduce the performance index value for buildings equipped with TMD. Ramezani *et al.* (2017) estimated optimal TMD parameters for a 15-degree of freedom structure based on designed fuzzy system and compared them to those parameters obtained from the Genetic algorithm and empirical relations.

Gravity Search Algorithm, GSA, is one of the newest optimization method introduced for the first time by (Rashedi *et al.* 2009). This method is a population-based approach where the researcher agents are included in the collection of masses as well as their interaction and the gravity force absorbs objects closely. Natural process of evolution is the basis of many optimization algorithms that can solve complex problems easily. GSA is one of the nature-inspired algorithms in various fields of civil engineering. For instance, Khajehzadeh *et al.* (2012) introduced a new version of GSA for non-linear constrained optimization of shallow foundation. They also, used the improved GSA in the optimization of RC retaining walls (Khajehzadeh *et al.* 2013). Khatibinia and Sadegh Naseralavi (2014) utilized Orthogonal Multi-Gravitational

\*Corresponding author, Professor

E-mail: [mzahrai@ut.ac.ir](mailto:mzahrai@ut.ac.ir)

<sup>a</sup>Ph.D. Candidate

E-mail: [nmirzai@ut.ac.ir](mailto:nmirzai@ut.ac.ir)

<sup>b</sup>Graduated Student

E-mail: [bozorgi.fatemeh@gmail.com](mailto:bozorgi.fatemeh@gmail.com)

Search Algorithm (OMGSA) as a meta-heuristic algorithm for optimizing the trusses on shape and sizing with frequency constraints. GSA has been used for damage detection as well by Daei *et al.* (2016). Adarsh and Janga Reddy (2015) used the GSA method for evaluating probabilistic design of canals with cross-sectional shape of horizontal bottom and parabolic sides. This algorithm lately has been used widely in various branches like computer science, electrical engineering, mechanical engineering as well for optimizing control and objective functions. For instance, Precup *et al.* (2012) applied a novel GSA for the optimal tuning of fuzzy controlled servo systems. (Rashedi *et al.* 2011) suggested a new linear and nonlinear filter modeling using GSA. In another research, Duman *et al.* (2012) used GSA method to find optimum solution for Optimal Power Flow (OPF).

Particle Swarm Optimization (PSO) is another nature-inspired algorithm as a random and evolutionary technique based on the simulation of the social behavior of animals during migration or searching for food. For the first time, PSO was presented by Kennedy and Eberhart (1995). Kennedy *et al.* (2001) also used PSO algorithm to evolve neural network weights and the network structure in some applications like diagnosing human tremor or metal removal procedure in environmental manufacturing. The application of PSO in the engineering field has an increasing pace, requiring very few parameters to be adjusted. PSO has been recently used in structural control and other fields in civil engineering. (Shariatmadar and Razavi 2014) used the combination of PSO and fuzzy logic controller (FLC) methods to optimize FLC parameters that minimize the displacement of top floor of an 11-story building with active tuned mass damper. In another research, a new optimization algorithm on the basis of PSO and charged system search (CSS) was offered by (Kaveh and Talatahari 2012) for optimum designing of structures. Also, Kaveh *et al.* (2015) used the combination of PSO and Swallow Swarm Optimization algorithm (SSO) and found better optimum solution in comparison with other optimization methods applied to highly dynamic truss shape. In addition, it has been used in electrical engineering to control the voltage of Japanese electric utility (Yoshida *et al.* 2000). Saravanan *et al.* (2007) found optimal location of transmission devices by using a PSO technique in order to obtain minimum cost which can be useful in rebuilding electrical devices. Also in another field of engineering, Ghashochi-Bargh and Sadr (2013) optimized the natural frequency of composite panels utilizing PSO algorithm and another method named finite strip method (FSM).

In this study, GSA and PSO algorithms are used to propose the optimal solution for obtaining the best value for damping ratio, stiffness and mass coefficient of TMD. Since the RD and AA have important roles in the failure of the structure, the aim of this article is to evaluate the optimum TMD parameters to reduce RD and AA while decreasing the values of the TMD parameters. Moreover, optimizing the TMD parameters provides an economical and practical design optimization approach for the buildings. A MATLAB code is developed in order to optimize the TMD parameters. To achieve an economical result, all of the TMD parameters

are variable. RD and AA are the criterion of the procedure. Two numerical examples from the literature are selected as a reference to compare the results with those of both GSA and PSO and to verify the code. To demonstrate the performance of the algorithm and efficiency of the presented approach, nine far-field and near-field earthquakes are also applied to the examples. The results showed that the proposed methods reduced the TMD parameters and structural responses.

## 2. Equations of motion

In this section, equations of motion for an n-story system with TMD installed on the top floor are given (Sabri *et al.* 2013).

For multiple degrees of freedom (MDOF) systems combined with TMD at the top floor subjected to ground, acceleration can be written as follows

$$M\ddot{x}(t) + C\dot{x}(t) + Kx(t) = P(t) \quad (1)$$

Where M, C and K are the mass, damping and stiffness matrices, respectively and  $x(t)$  is also the vector of horizontal displacements given as follows

$$M = \begin{bmatrix} m_1 & 0 & \dots & 0 & 0 \\ 0 & m_2 & \dots & 0 & 0 \\ \cdot & \cdot & \cdot & \cdot & \cdot \\ \cdot & \cdot & \cdot & \cdot & \cdot \\ 0 & 0 & \dots & m_n & 0 \\ 0 & 0 & \dots & 0 & m_d \end{bmatrix} \quad (2)$$

$$C = \begin{bmatrix} (c_1 + c_2) & -c_2 & \dots & & \\ -c_2 & (c_2 + c_3) & \dots & & \\ \cdot & \cdot & \cdot & \cdot & \cdot \\ \cdot & \cdot & \cdot & \cdot & \cdot \\ & & \dots & (c_n + c_d) & -c_d \\ & & \dots & -c_d & c_d \end{bmatrix} \quad (3)$$

$$K = \begin{bmatrix} (k_1 + k_2) & -k_2 & \dots & & \\ -k_2 & (k_2 + k_3) & \dots & & \\ \cdot & \cdot & \cdot & \cdot & \cdot \\ \cdot & \cdot & \cdot & \cdot & \cdot \\ & & \dots & (k_n + k_d) & -k_d \\ & & \dots & -k_d & k_d \end{bmatrix} \quad (4)$$

$$x(t) = [x_1 \quad x_2 \quad \dots \quad x_n \quad x_d]^T \quad (5)$$

$m_i$ ,  $c_i$ ,  $k_i$  and  $x_i$  are mass, damping coefficient, stiffness and horizontal displacement of the  $i$ th story of a building ( $i=1, 2, \dots, n$ ).  $m_d$ ,  $c_d$  and  $k_d$  are the mass, damping coefficient and the stiffness of the TMD installed on the top of the building

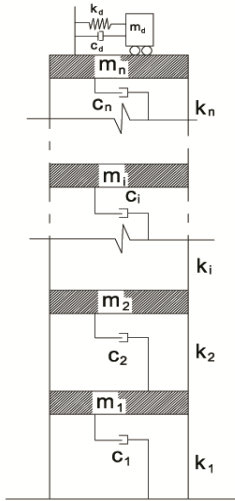


Fig. 1 MDOF system with a single TMD on the top floor

as shown in Fig. 1.

$x_d$  is the displacement of TMD related to the ground. The displacement vector can be written as follows (Clough and Penzien 1993)

$$x = \phi_1 Y_1 + \phi_2 Y_2 + \dots + \phi_n Y_n \quad (6)$$

and in the matrix notation:

$$x = \phi Y \quad (7)$$

Where  $\phi$  is the mode-shape matrix and  $Y$  is the generalized coordinate vector such that  $n \times n$  mode shape matrix, transforms generalized coordinate vector,  $Y$ , to the geometric coordinates vector  $x$ . The mode-shape matrix is non-singular that can be inverted. By pre-multiplying the Eq. (1) by  $\phi_i^T$  and combining it with Eq. (7), Eq. (8) is obtained as follows

$$\phi_i^T M \phi \ddot{Y}(t) + \phi_i^T C \phi \dot{Y}(t) + \phi_i^T K \phi Y(t) = \phi_i^T P(t) \quad (8)$$

According to the orthogonality principle, all components with  $i \neq j$  are omitted and the Eq. (8) can be written as

$$M_i \ddot{Y}_i(t) + C_i \dot{Y}_i(t) + K_i Y_i(t) = P_i(t) \quad (9)$$

or in other words

$$\ddot{Y}_i(t) + 2\xi_i \omega_i \dot{Y}_i(t) + \omega_i^2 Y_i(t) = P_i(t) / M_i \quad (10)$$

in which

$$P_i(t) = -M \{1\} \ddot{x}_g(t) \quad (11)$$

And  $M_i$ ,  $C_i$ ,  $K_i$  and  $Y(t)$  are generalized mass, damping, stiffness and displacement, respectively for the  $i$ th normal mode (Clough and Penzien 1993).

### 3. GSA algorithm

GSA is a new optimization theory developed based on gravity law for continuous optimization problems. In GSA,

each factor contains four parameters: position, inertial mass, active gravitational mass and passive gravitational mass.

The solution to the problem is presented by the position of the mass, where a fitness function is employed to determine the gravitational masses as well as the inertial ones. So as to steer the algorithm, both the gravitational and the inertial masses are adjusted, while each mass puts forward a solution.

The heaviest mass, leads to the attraction of masses. Therefore, the best possible solution is provided by the heaviest mass in the search space. There are several steps for the GSA as follows (Sabri *et al.* 2013):

Step One: Initialization of the agents:

The positions of the number of agents ( $N$ ) are initialized at random.

$$X_i = (x_i^1, \dots, x_i^d, \dots, x_i^n), \text{ for } i = 1, 2, \dots, N. \quad (12)$$

$x_i^d$  stands for the positions of the  $i$ th agent in the  $d$ th dimension, whereas  $n$  represents the dimension of space.

Step Two: Fitness evolution and computation of the best fitness:

In each iteration, the fitness evolution is conducted through the evaluation of the best and worst fitness for all the agents meant for the problems of minimization or maximization.

Problems of minimization

$$\begin{aligned} best(t) &= \min fit_j(t) \\ j &\in (1, \dots, N) \end{aligned} \quad (13)$$

$$\begin{aligned} worst(t) &= \max fit_j(t) \\ j &\in (1, \dots, N) \end{aligned} \quad (14)$$

Problems of maximization

$$\begin{aligned} best(t) &= \max fit_j(t) \\ j &\in (1, \dots, N) \end{aligned} \quad (15)$$

$$\begin{aligned} worst(t) &= \min fit_j(t) \\ j &\in (1, \dots, N) \end{aligned} \quad (16)$$

$fit_j(t)$  is the fitness value of the agent  $j$ th at the iteration  $t$ . The best and worst fitness at the iteration  $t$  are also illustrated via the symbols of  $best(t)$  and  $worst(t)$ .

Step Three: Calculating of the gravitational constant ( $G$ ):

$G$  as the gravitational constant is calculated at the iteration  $t$

$$G(t) = G_0 e^{(-\alpha t/T)} \quad (17)$$

At the beginning,  $G_0$  and  $\alpha$  are initialized. However, they will be reduced by time in order to control the search precision.  $T$  represents the entire number of iterations.

Step Four: Computation of the masses of agents:

At the iteration  $t$ , the gravitational masses as well as the inertial ones are computed for each agent (Sabri *et al.* 2013)

and are updated by the Eqs. (9) and (20)

$$M_{ai} = M_{pi} = M_{ii} = M_i \quad i = 1, 2, \dots, N \quad (18)$$

$$m_i(t) = \frac{fit_i(t) - worst(t)}{best(t) - worst(t)} \quad (19)$$

$$M_i(t) = \frac{m_i(t)}{\sum_{j=1}^N m_j(t)} \quad (20)$$

$M_{ai}$  and  $M_{pi}$  show in turn the gravitational masses in the active and passive forms, while  $M_{ii}$  stands for the inertial mass of the agent  $i$ th. Also,  $fit_i(t)$  indicates the fitness associated with mass  $i$  in time  $t$ .

Step Five: Computation of the accelerations of agents:

At the iteration  $t$ , the acceleration of the  $i$ th agents is calculated

$$a_i^d(t) = F_i^d(t) / M_{ii}(t) \quad (21)$$

$F_i^d(t)$  represents the total force applying on agent  $i$ th which is calculated as follows

$$F_i^d(t) = \sum_{j \in Kbest, j \neq i} rand_j F_{ij}^d(t) \quad (22)$$

The arrangement of the first  $K$  agents with the best fitness value and the biggest mass is called the Kbest.

There will be a linear reduction in the Kbest over time. Furthermore, there will be only one agent which implies force to other agents in the last part.

$F_{ij}^d(t)$  is calculated via Eq. (23)

$$F_{ij}^d(t) = G(t) \frac{M_{pi}(t) \times M_{\alpha j}(t)}{R_{ij}(t) + \varepsilon} (x_j^d(t) - x_i^d(t)) \quad (23)$$

$F_{ij}^d(t)$  represents the force acting on the agent  $i$  from the agent  $j$  at the dimension of  $d$ th and the iteration of  $i$ th.

$R_{ij}(t)$  stands for the distance of Euclidian between the two agents of  $i$  and  $j$  at the iteration  $t$ .

$G(t)$  indicates the calculated gravitational constant in an equal iteration whereas  $\varepsilon$  is just a small constant.

Step Six: Positions of agents and velocity:

The following equations are used to calculate the position and the velocity of the agents at the succeeding iteration ( $t+1$ )

$$v_i^d(t+1) = rand_i \times v_i^d(t) + a_i^d(t) \quad (24)$$

$$x_i^d(t+1) = x_i^d(t) + v_i^d(t+1) \quad (25)$$

Step Seven: Repetition of the Steps 2 to 6

In the final step, steps Two to Six need to be repeated till the iterations get to their maximum extent. The overall fitness is computed as the greatest fitness value at the ultimate iteration while the global solution to that specific

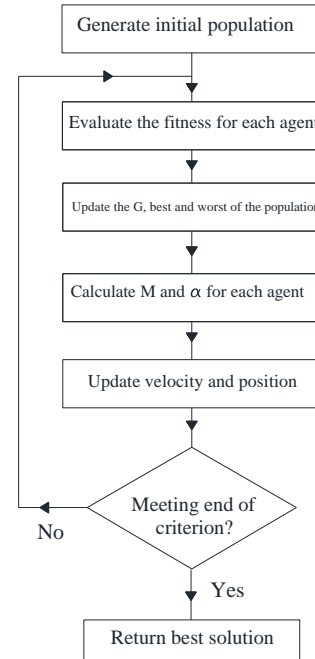


Fig. 2 GSA flowchart (Sabri *et al.* 2013)

problem is calculated as the position of the matching agent at particular dimensions (Sabri *et al.* 2013). The flowchart of GSA is illustrated in Fig. 2.

#### 4. PSO algorithm

Particle Swarm Optimization is a biological search method that simulates social behaviors of migratory birds or a group of fish searching for food. Each member of this community can benefit from its own discoveries and experiences of all members in order to gradually approach the optimal (Kennedy and Eberhart 1995).

PSO begins with a group of particle swarms that updates the situations for finding the best optimum solution. Each particle randomly takes the initial values (the location of each member of the group that birds are looking for food). The algorithm finds the optimal solution to the problem by directing these values during successive iterations.

In fact, the movement of birds in this algorithm depends on two factors: the individual and the social movement. The combination of these two movements creates a model to find the best target point in optimization problems.

Each particle keeps the best solution that has achieved by that particle up until now. This value is called personal best or Pbest. Another best value that is followed by the PSO is the best value obtained by any particle in the neighborhood of that particle up until now. This value is called Gbest.

The fitness function is investigated for each particle in the current position. If it is larger than Pbest, then Pbest will be updated. If it is larger than Gbest, then Gbest will be updated. The general view of Pbest and Gbest has been shown in Fig. 3. After finding the above-mentioned values,

the movement speed of particles, as well as their next place are calculated from the following formulas (Kennedy and Eberhart 1995)

$$V_i(t+1) = \omega V_i(t) + c_1 r_1 (Pbest_i - x_i(t)) + c_2 r_2 (Gbest - x_i(t)) \quad (26)$$

$$x_i(t+1) = x_i(t) + v_i(t+1) \quad (27)$$

Where  $V_i$  and  $x_i$  are the velocity and the place of the  $i$ th particle, respectively,  $t$  represents the time step,  $\omega$  is the inertia weight,  $c_1$  and  $c_2$  are individual and social learning factors which are usually equal two,  $r_1$  and  $r_2$  take randomly values between 0 and 1.  $Pbest$  and  $Gbest$  parameters were defined before.

The velocity vector of each particle in PSO algorithm is updated and then a new speed is added to the last position of the particle.

The PSO flowchart as illustrated in Fig. 4 is used in this study to propose optimum parameters of TMD.

## 5. GSA and PSO algorithms for optimization of TMDs

In this study, the MATLAB codes are used for linear dynamic analysis. The constraint of optimization problem in this study is limitation of allowable drifts based on design codes. At first, an objective function and the number of iterations are determined. The objective functions for the first and second examples are defined as Eqs. (30) and (31), respectively.

The  $H_2$  norm is clarified as the root mean square of system impulse response which can be further defined as an average system taken over all frequencies. It is given by Eq. (28) (Hadi and Arfiadi 1998)

$$\|T_{rw}\|_2 = \sqrt{\frac{1}{2\pi} \int_{-\infty}^{+\infty} \text{Trace}(T_{rw}(j\omega)T_{rw}^*(j\omega)) d\omega} \quad (28)$$

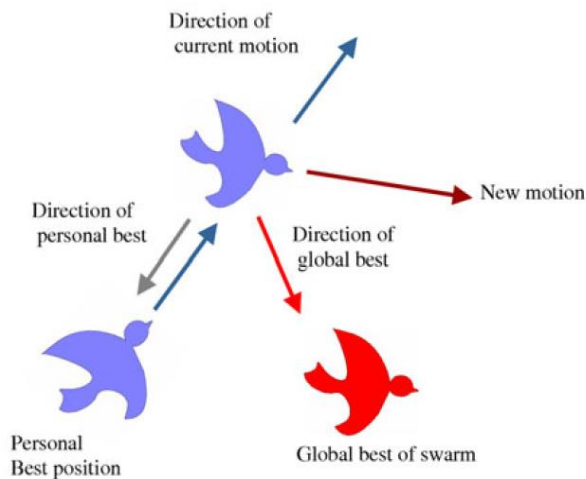


Fig. 3 A general view of pbest and gbest of the PSO algorithm (Ahmadi et al. 2010)

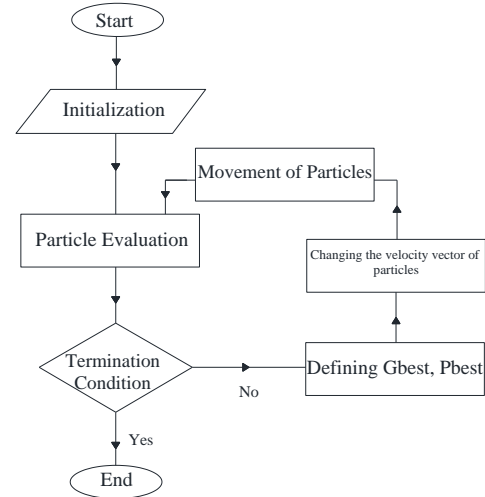


Fig. 4 The PSO flowchart

Where the parameters are defined as follows:

$\|T_{rw}\|_2 = H_2$  norm transfer function from external perturbation  $w$  to the controlled output  $r$ .

$\omega$  = frequency,  $j$  = imaginary number,  $*$  = complex conjugate transpose

For the systems with controlled output

$$r = C_w Z \quad (29)$$

The  $H_2$  norm transfer function from  $w$  to  $r$  can be calculated by

$$\|T_{rw}\|_2 = [\text{Trace}(C_w L_c C_w^T)]^{0.5} = [\text{Trace}(E^T L_0 E)]^{0.5} \quad (30)$$

Where  $L_c$  and  $L_0$  are the controllability and the observability Gramians, respectively.

The objective function for the second example adopted from (Farshidianfar and Soheili 2013) is defined as Eq. (31)

$$F = \ddot{U}_{\max} + 10U_{\max} \quad (31)$$

where  $F$ ,  $\ddot{U}_{\max}$  and  $U_{\max}$  indicate the objective function, maximum acceleration and maximum displacement, respectively.

The optimizer code generates three values for TMD parameters (mass, stiffness and damping ratio) which are variable. These parameters are called by the analyst code and are used to analyze the structure. As soon as the structure is analyzed, the responses are sent to the optimizer code again and the objective function is checked. Finally, other values are chosen. These stages continue until the iterations end. The last response is the best answer that minimize the objective function. The flowchart of this process is observable in Fig. 5.

## 6. Numerical examples

In this section, two key examples are used from literature to show the performance of the proposed

algorithms. For this reason, the optimum estimation of TMD parameters obtained from GSA and PSO methods are compared with some other methods used in references. A MATLAB program is composed for the time history analysis.

### 6.1 Example 1

The example No. 1 is a 40-story shear building with a TMD on the top floor, used by (Farshidianfar and Soheili 2013). The total mass of the stories is  $9.8e5$  kg and the stiffness of all the 40 floors is as follows

$$\begin{aligned} K_1 &= 213e7 \text{ (N/m)} & i &= 1 \\ K_i &= 213e7-3(i-1) \text{ (N/m)} & 2 \leq i &\leq 40 \end{aligned} \quad (32)$$

The damping coefficients are also

$$\begin{aligned} C_i &= 0.02K_i \text{ (N.s/m)} & 1 \leq i &\leq 39 \\ C_i &= 0.02004K_i \text{ (N.s/m)} & i &= 40 \end{aligned} \quad (33)$$

And the height of the stories is 4 m. Since the maximum RD of the stories is an important item for the structural analysis, most researchers in this field aim to reduce the maximum RD and AA. The method used by Farshidianfar

and Soheili is the Ant Colony algorithm. The interval of design variables in this example is  $1500 \leq m \leq 3037.97$  ton;  $1300 \leq K \leq 1547.72$  kN/m;  $80 \leq C \leq 173.55$  kN.s/m. Finally, the optimized parameters obtained as  $m=1547.720$  ton,  $K=3037.970$  kN/m and  $C=173.55$  kN.s/m.

To validate the code and compare it to results obtained by Farshidianfar and Soheili, the 1978 Tabas earthquake, Iran (RSN 143, Tabas station) is applied to the structure.

Table 1 shows the values of RD and AA for the structure in the absence of TMD for verification. Moreover, the effect of the GSA and PSO on the RD and AA is illustrated.

Table 2 shows the reduction percentage for all mentioned methods. The maximum RD is related to the 38<sup>th</sup> floor in GSA and the 40<sup>th</sup> floor in the PSO algorithm while it seems the maximum RD for Ant Colony algorithm (used reference) is related to the 40<sup>th</sup> floor. Hence, Table 3 presents the maximum RD values under the Tabas Earthquake for all of the stories.

Table 3 illustrates that TMD can reduce the RD in all stories. The top story displacement is important in tall buildings. As observed, the RD reduction at the top floor is more than that in the bottom floors, showing the positive effect of TMD. Maximum reduction is related to the 40<sup>th</sup> floor with the GSA and the 36<sup>th</sup> floor with the PSO algorithm with reduction percentage of 37% and 36.5%,

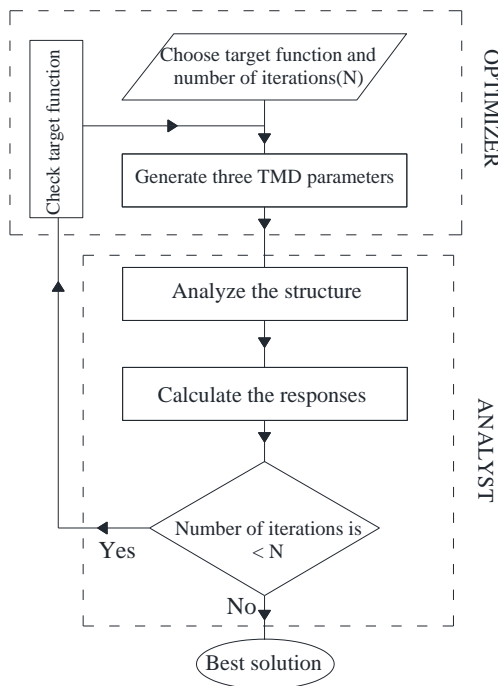


Fig. 5 Flowchart showing how the analyst and optimizer codes work

Table 2 The reduction percentage for three algorithms under the Tabas earthquake (Ex. 1)

Algorithms	Displacement reduction (%)	Absolute acceleration reduction (%)
Ant colony	30.14	0.19
GSA	37.01	0.31
PSO	35.96	0.38

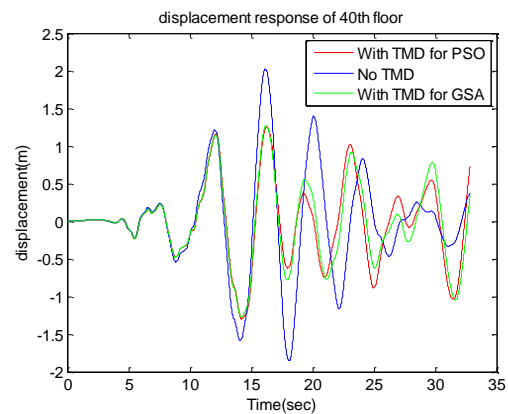


Fig. 6 Relative displacement (RD) response of the 40<sup>th</sup> floor under the Tabas earthquake (Ex. 1)

Table 1 The maximum relative displacement (RD) and the absolute acceleration (AA) under the 1978 Tabas earthquake (Ex. 1)

	Ant colony		GSA		PSO	
	$U_{40}$ (cm)	$\ddot{U}_{\max-rel}$ (cm/s <sup>2</sup> )	$U_{40}$ (cm)	$\ddot{U}_{\max-rel}$ (cm/s <sup>2</sup> )	$U_{\max}$ (cm)	$\ddot{U}_{\max-rel}$ (cm/s <sup>2</sup> )
Without TMD	2.0235	12.7756	2.0241	12.7727	2.0241	12.7727
With TMD	1.4135	12.7507	1.2749	12.7321	1.2963	12.7248



Table 3 Maximum relative displacements (RD) (m) under the 1978 Tabas earthquake (Ex.1)

Story No.	No TMD	Proposed method (GSA)	Reduction (%)	Proposed method (PSO)	Reduction (%)
1	0.0626	0.0485	22.51	0.0486	22.36
2	0.1259	0.0965	23.35	0.0967	23.19
3	0.1898	0.1439	24.16	0.1443	23.97
4	0.2542	0.1906	25.01	0.1913	24.74
5	0.3191	0.2366	25.86	0.2374	25.60
6	0.3844	0.2817	26.72	0.2828	26.43
7	0.4500	0.3261	27.53	0.3272	27.29
8	0.5162	0.3704	28.24	0.3708	28.17
9	0.5827	0.4140	28.95	0.4144	28.88
10	0.6497	0.4572	29.63	0.4577	29.55
11	0.7172	0.4994	30.36	0.5000	30.28
12	0.7847	0.5422	30.90	0.5413	31.02
13	0.8523	0.5885	30.95	0.5814	31.78
14	0.9198	0.6346	31.01	0.6208	32.51
15	0.9869	0.6802	31.08	0.6626	32.86
16	1.0533	0.7251	31.15	0.7065	32.93
17	1.1182	0.7689	31.24	0.7493	32.99
18	1.1821	0.8115	31.35	0.7911	33.08
19	1.2446	0.8528	31.48	0.8317	33.18
20	1.3056	0.8925	31.64	0.8708	33.30
21	1.3646	0.9308	31.79	0.9085	33.42
22	1.4217	0.9674	31.95	0.9448	33.54
23	1.4770	1.0021	32.16	0.9794	33.69
24	1.5303	1.0352	32.35	1.0122	33.86
25	1.5814	1.0665	32.56	1.0435	34.01
26	1.6303	1.0957	32.79	1.0727	34.20
27	1.6765	1.1228	33.03	1.1002	34.38
28	1.7205	1.1482	33.27	1.1257	34.57
29	1.7623	1.1714	33.53	1.1491	34.80
30	1.8016	1.1926	33.80	1.1707	35.02
31	1.8385	1.2117	34.09	1.1901	35.27
32	1.8727	1.2285	34.40	1.2072	35.54
33	1.9041	1.2431	34.72	1.2221	35.82
34	1.9324	1.2552	35.04	1.2346	36.11
35	1.9574	1.2648	35.39	1.2448	36.41
36	1.9789	1.2716	35.74	1.2559	36.54
37	1.9965	1.2756	36.11	1.2695	36.41
38	2.0100	1.2767	36.48	1.2816	36.24
39	2.0193	1.2747	36.87	1.2907	36.08
40	2.0241	1.2749	37.01	1.2963	35.96
TMD	-	6.9309	----	7.3784	----
Mean Value			31.41		32.15

respectively. The average reduction percentage is 31.4% for the GSA and 32.2% for the PSO.

Moreover, reducing the TMD parameters is more practical and economical. For this reason, it is tried to achieve the least values for the mass, stiffness and damping ratio. The values of TMD parameters are listed in Table 4.

Table 4 illustrates that the proposed methods have caused a reduction in the TMD parameters compared to the Ant colony method. As presented, the GSA could reduce stiffness, damping coefficient and mass by 29.24%, 47.69 and 1.88% while PSO could reduce them by 23.29%, 47.30% and 2.11%, respectively. As follows, the displacement response of the 40th floor is shown for the Tabas earthquake in Fig. 6. It can be found from this figure that using TMD could reduce the peak values by 36.5% for the GSA and by 36% for the PSO.

Since the story drift has an important role in the structural failure, the drift diagram must be studied. Fig. 7 shows that the drifts of all stories are in the range of 0.0034 to 0.0121 for both algorithms approximately demonstrating a more relatively uniform distribution. It means that all stories have somehow similar contributions in total building displacement showing an optimum scenario. For this purpose, standard deviation (SD) as an index is employed to evaluate the dispersion of story drifts as Eq. (34)

$$\sigma = \sqrt{\frac{1}{N} \sum_{i=1}^N (x_i - \mu)^2} \quad (34)$$

Where

$$\mu = \frac{1}{N} \sum_{i=1}^N x_i \quad (35)$$

The values of SD are listed in Table 5. These values demonstrate that the PSO algorithm has better performance in the case of uniform deformation.

After employing the optimization algorithm, the optimized parameters are fixed and then the performance of the structure equipped with the same TMD is evaluated under different far and near field earthquakes. Therefore, some well-known ground motions from all over the world have been applied to the structure with and without the optimized TMD. Some of these earthquakes were selected from near-

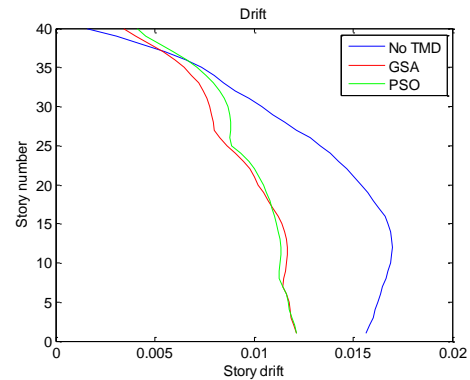


Fig. 7 Story drift for example 1 under the Tabas earthquake (Ex.1)

Table 4 The reduction percentage of TMD parameters (Ex.1)

	Farshidinfar and Soheili (AC)	Proposed Method (GSA)	Reduction (%)	Proposed Method (PSO)	Reduction (%)
Stiffness (kN/m)	3037.970	2149.624	29.24	2330.444	23.29
Damping coefficient (kN.s/m)	173.554	90.79254	47.69	91.455	47.30
Mass (ton)	1547.720	1518.693	1.88	1515.054	2.11

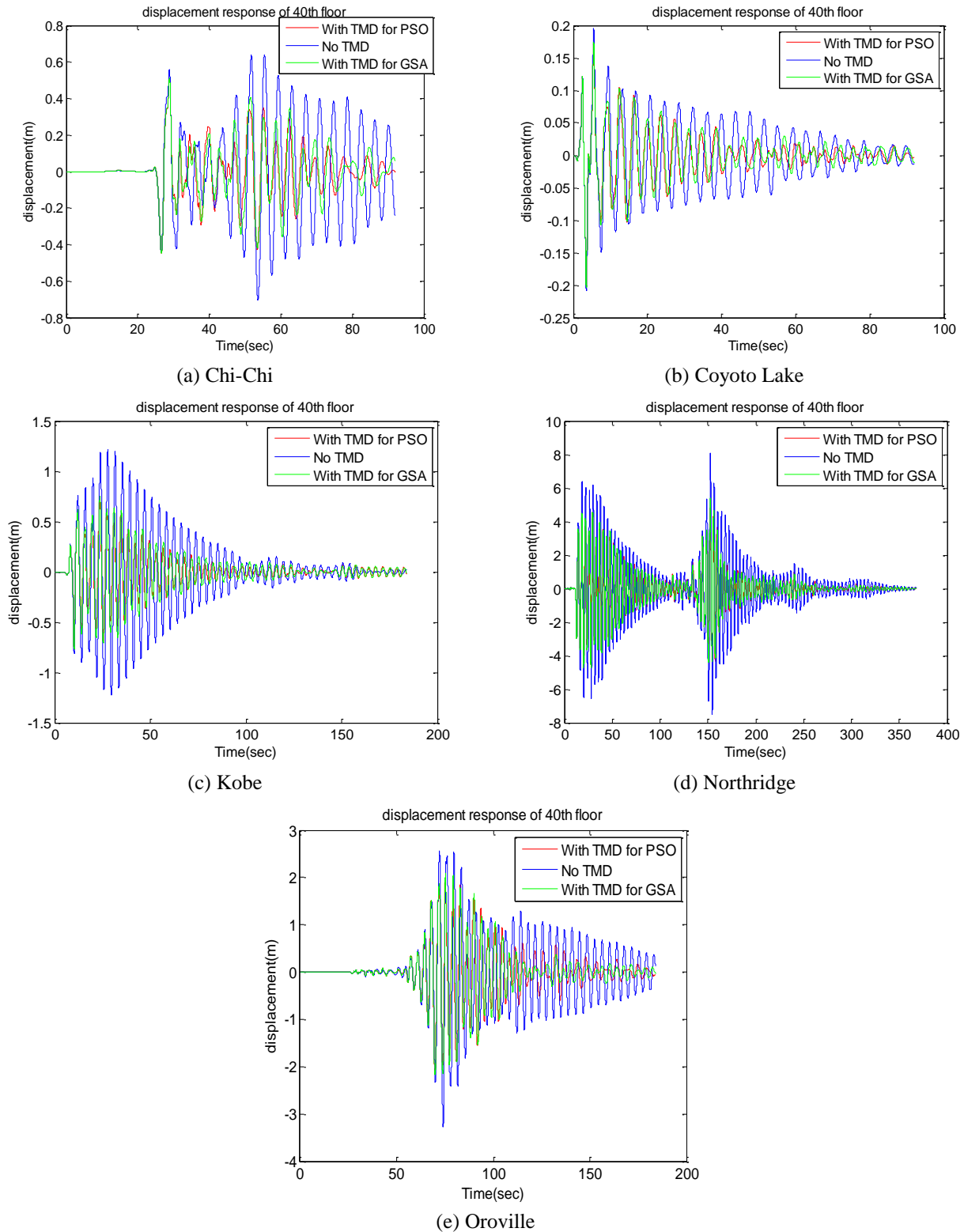


Fig. 8 Response of the 40th story under the Near-field records (Ex. 1)



Table 5 Standard deviation for story drifts in the 1<sup>st</sup> example

Structure	Standard deviation
Optimized TMD by GSA	0.003956115
Optimized TMD by PSO	0.00336041
Structure without TMD	0.004718042

field stations and the others from far-field ones to investigate the effect of both types of the ground motions. In order to make them easily accessible, the RSN (Record Station Number) of each record has been presented. The displacement results are shown in Figs. 8 and 9 for near-field and far-field earthquakes, respectively. These figures demonstrate that the TMD has a positive effect on the building.

The values of the max RD ( $U_{\max}$ ) and max AA ( $\ddot{U}_{\max}$ ) have been listed in the Tables 6 and 7 for all mentioned earthquakes. Based on Table 6, results show that the TMD can reduce the RD up to 43.82% by GSA and 50.54% by PSO algorithm.

Table 7 shows that the TMD with mentioned optimum parameters has the positive effect on the AA, as well. In some cases, the absolute acceleration has reduced up to

21.3% for the GSA and 25.2% for the PSO algorithm. Note that the absolute acceleration is calculated as:

$$\ddot{U}_{\max} = \ddot{U}_{\max-rel} + \ddot{U}_g \quad (36)$$

## 6.2 Example 2

Specifications of the second example which is gained from (Sadek *et al.* 1997) are listed in Table 8. This structure is a 10-story building where the height of the stories is assumed 3 m. The mass, stiffness and damping coefficient of all the stories are as Hadi and Arfiadi (1998) who considered  $m=55.45$  ton,  $K=437.9$  kN/m and  $C=47.9$  kN.s/m. The interval of design variables in this example is  $20 \leq m \leq 50$  ton;  $150 \leq K \leq 220$  kN/m;  $20 \leq C \leq 60$  kN.s/m. The responses of this building under the Imperial Valley Irrigation District (El-Centro) 1940 NS ground acceleration record are presented in Table 9.

As mentioned before, the reduction of the RD is an important factor for the structural analysis. In this study, the maximum RD under the El-Centro earthquake is related to the top floor with 0.281, 0.272, 0.2403, 0.2378 based on

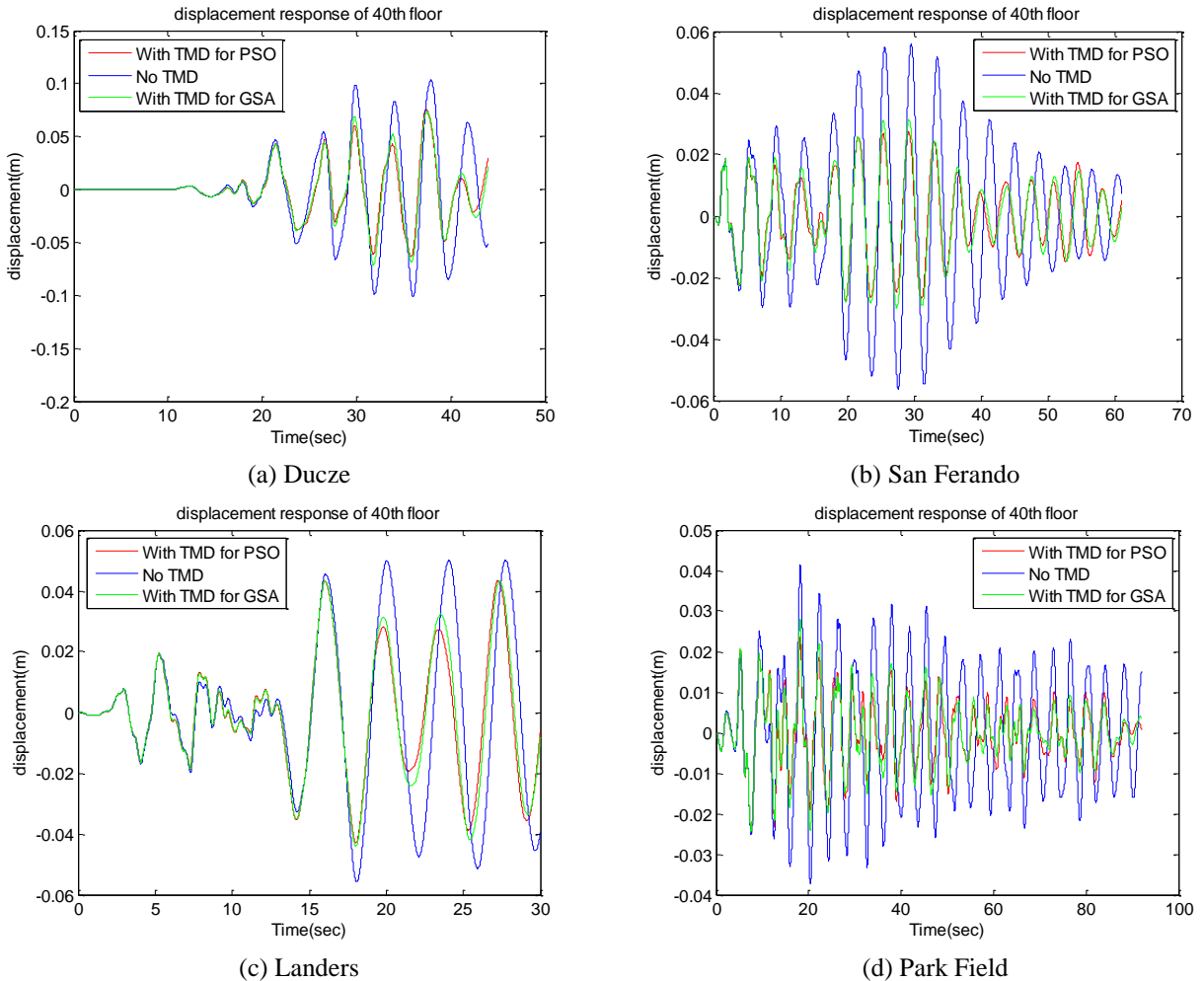


Fig. 9 Response of the 40th story under the Far-field records (Ex. 1)

Table 6 Maximum relative displacement (RD) (m) (Ex. 1)

	Records	No TMD	GSA		PSO	
		$U_{\max}$	$U_{\max}$	Reduction (%)	$U_{\max}$	Reduction (%)
Near-Field Records	Chi-Chi-RSN 1549	0.7050	0.5121	27.36	0.5145	27.03
	Coyoto Lake-RSN 150	0.2079	0.2026	2.56	0.2022	2.76
	Kobe-RSN 1120	1.2249	0.7666	37.42	0.7647	37.57
	Northridge-RSN 1120	8.0662	5.4065	32.97	4.8089	40.38
	Oroville-RSN 119	3.2649	2.1988	32.65	2.1475	34.22
Far-Field Records	San Ferando-RSN 63	0.0562	0.0316	43.82	0.0278	50.54
	Ducze-RSN 1613	0.1034	0.0733	29.15	0.0755	26.96
	Landers-RSN 3752	0.0558	0.0440	21.16	0.0435	22.12
	Park Field-RSN 4150	0.0415	0.0280	32.57	0.0243	41.58

Table 7 Maximum absolute acceleration ( $\text{m/s}^2$ ) (Ex.1)

	Records	No TMD	GSA		PSO	
		$\ddot{U}_{\max}$	$\ddot{U}_{\max}$	Reduction (%)	$\ddot{U}_{\max}$	Reduction (%)
Near-Field Records	Chi-Chi-RSN 1549	7.7407	7.7396	0.01	7.7395	0.01
	Coyoto Lake-RSN 150	3.9049	3.9029	0.05	3.9008	0.10
	Kobe-RSN 1120	4.9311	4.8453	1.74	4.8369	1.91
	Northridge-RSN 1120	30.5266	24.0369	21.26	22.8449	25.16
	Oroville-RSN 119	14.2435	13.1046	8.00	12.7665	10.37
Far-Field Records	San Ferando-RSN 63	0.5869	0.5869	0.00	0.5869	0.00
	Ducze-RSN 1613	0.4725	0.4724	0.02	0.4724	0.02
	Landers-RSN 3752	0.6462	0.6459	0.05	0.6458	0.05
	Park Field-RSN 4150	0.3061	0.3052	0.28	0.3052	0.29

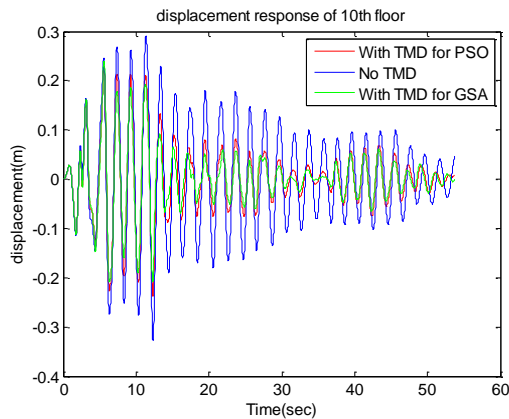


Fig. 10 Displacement response of top floor of the 10-story building under the El-Centro earthquake (Ex. 2)

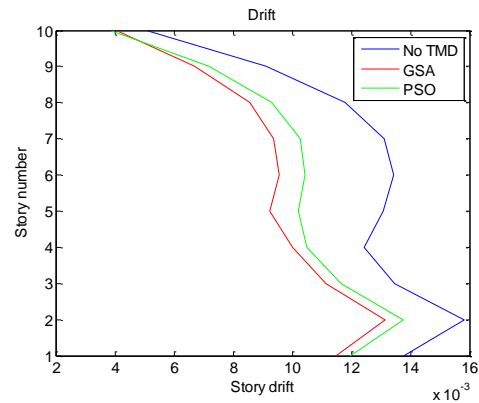


Fig. 11 Story drift for the 10-story building under the El-Centro earthquake (Ex. 2)

(Sadek *et al.* 1997), GA, GSA and PSO algorithms, respectively demonstrating 14.1, 16.8, 26.5 and 27.3% reduction. Therefore, it can be found out that the PSO algorithm can reduce the displacement of the top story more than the other mentioned methods while highest average reduction is related to GSA with 20.7%.

About the TMD parameters, the proposed methods could reduce the TMD parameters 50.5, 29.1 and 26.4, by GSA and 63.2, 18.5 and 9.7% by PSO for stiffness,

damping ratio and mass, respectively compared to the GA method as shown in Table 10. This means that the TMD with the optimized parameters could reduce the RD and AA while it has less mass and is thus more economical than the TMD proposed by Hadi and Arfiadi and Lee *et al.*

It is worth to mention that the responses of the top stories have been reduced up to 10%, affecting directly on the story drifts (Fig. 10). As shown in Fig. 11 the GSA and PSO algorithms have the maximum reduction percentage up to 29.5 and 24.1%.

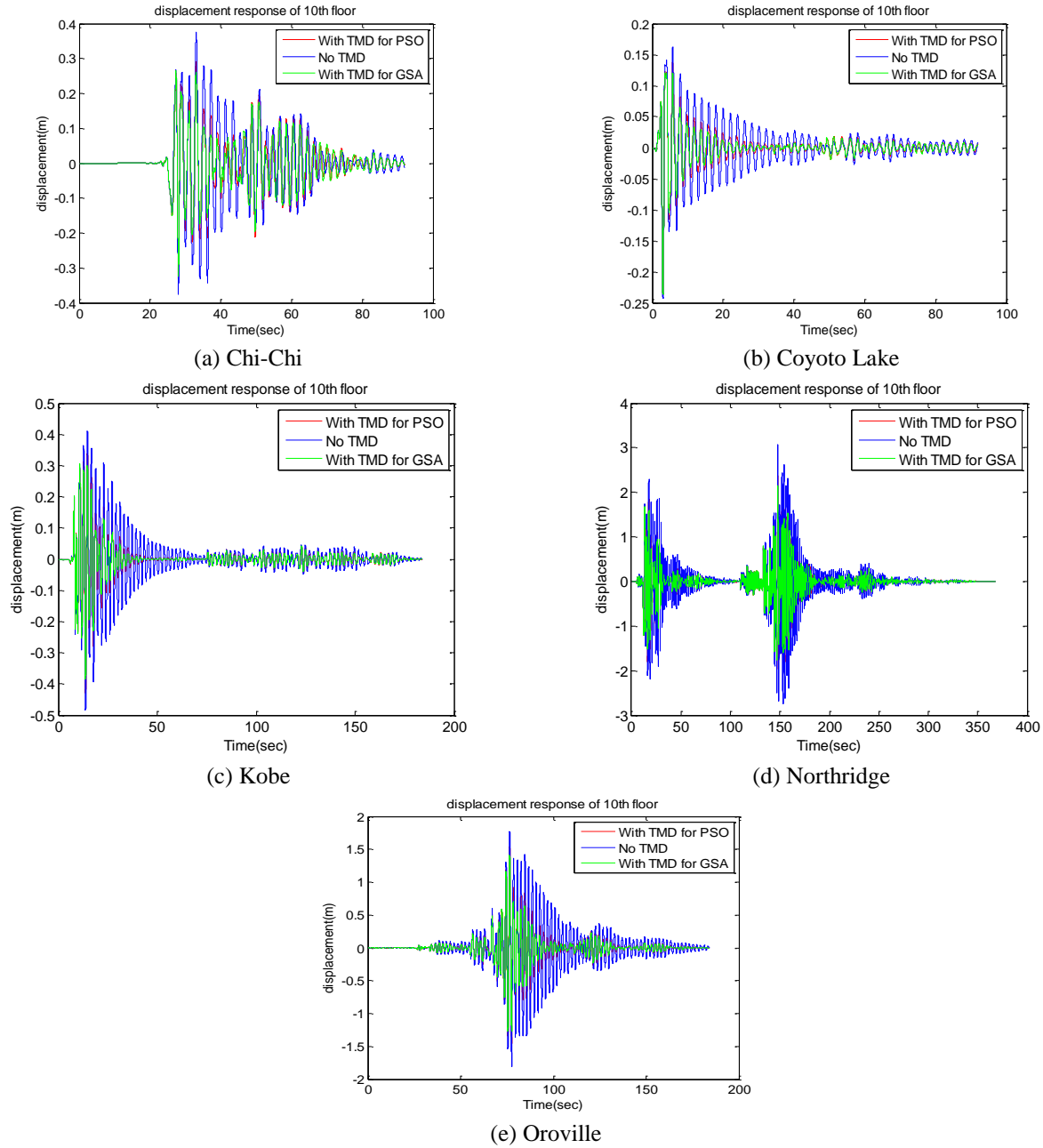


Fig. 12 Top floor displacement for the 10-story building under the Near-field records (Ex. 2)

Table 8 Specification of the building (Ex. 2)

Story number	Mass (ton)	Stiffness (kN/m)	Damping (kN.s/m)
1	179	62470	805.863
2	170	52260	674.154
3	161	56140	724.206
4	152	53020	683.958
5	143	49910	643.839
6	134	46790	603.591
7	125	43670	563.343
8	116	40550	523.095
9	107	37430	482.847
10	98	34310	442.599

The deformation uniformity index, Eqs. (34) and (35), are used to compare the performance of each algorithm. The results are listed in Table 11. The results show that GSA algorithm is more efficient.

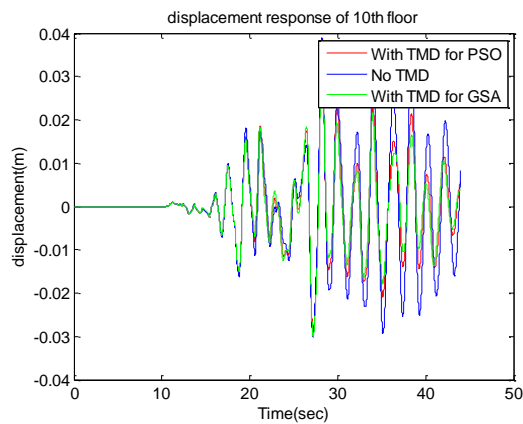
In order to show the efficiency of the methods, the selected well-known ground motions were applied to this building, too (Figs. 12 and 13). The same optimized parameters of TMD are used for all earthquakes. The maximum RD and AA are listed in Tables 12 and 13. The results show that the values of RD and AA have been decreased under all ground motions. As obtained, RD has reduced up to 29.7% by the GSA and 22.4% by the PSO. AA has also reduced about 29.1% by the GSA and 21.7% by the PSO algorithm.

Table 9 Maximum relative displacements (RD) (m) under the 1940 El Centro NS earthquake (Ex. 2)

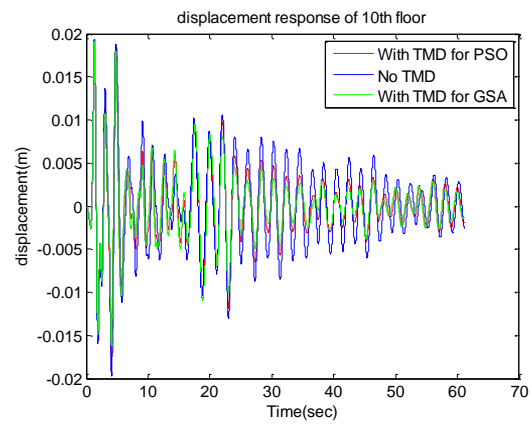
Story No.	No. TMD	Sadek <i>et al.</i> 1997	Reduction (%)	Hadi and Arfiadi (GA)	Reduction (%)	Proposed method (GSA)	Reduction (%)	Proposed method (PSO)	Reduction (%)
1	0.041	0.036	12.195	0.034	17.073	0.0343	16.3031	0.0358	12.683
2	0.088	0.077	12.500	0.072	18.182	0.0737	16.276	0.0770	12.500
3	0.129	0.113	12.403	0.105	18.605	0.1070	17.056	0.1118	13.333
4	0.166	0.145	12.651	0.134	19.277	0.1369	17.518	0.1433	13.675
5	0.197	0.172	12.690	0.16	18.782	0.1617	17.932	0.1696	13.909
6	0.222	0.194	12.613	0.184	17.117	0.1805	18.698	0.1900	14.414
7	0.252	0.219	13.095	0.21	16.667	0.1934	23.259	0.2048	18.730
8	0.286	0.245	14.336	0.236	17.483	0.2101	26.530	0.2149	24.860
9	0.313	0.266	15.016	0.258	17.572	0.2286	26.965	0.2285	26.997
10	0.327	0.281	14.067	0.272	16.820	0.2403	26.523	0.2378	27.278
TMD	—	0.456		0.635		0.4793		0.2982	
Mean value			13.15%		17.75%		20.7%		17.83%

Table 10 Reduction percentage of TMD parameters (Ex. 2)

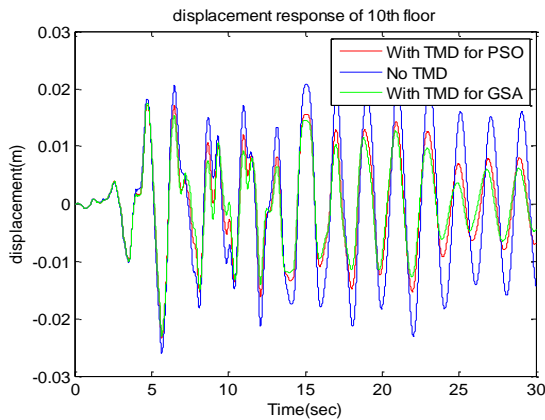
	Hadi and Arfiadi (GA)	Proposed Method (GSA)	Reduction (%)	Proposed Method (PSO)	Reduction (%)
Stiffness(kN/m)	437.9	216.67	50.5	161.335	63.2
Damping(kN.s/m)	47.9	33.94	29.1	39.024	18.5
Mass(ton)	55.45	40.81	26.4	50.076	9.7



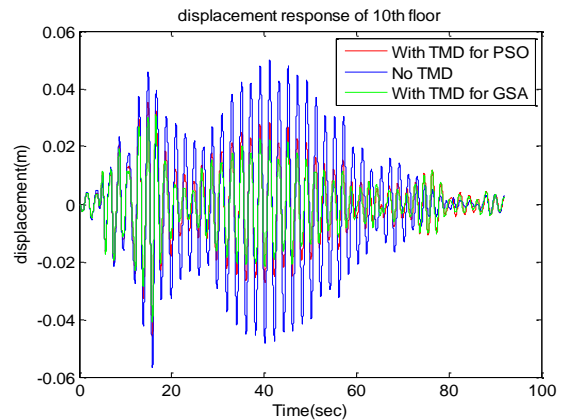
(a) Ducez



(b) San Fernando



(c) Landers



(d) Park Field

Fig. 13 Response of top floor for the 10-story building under the Far-field records (Ex.2)

Table 11 Standard deviation for story drifts in the 2<sup>nd</sup> example

Structure	Standard deviation
Optimized TMD by GSA	0.002540994
Optimized TMD by PSO	0.002729112
Structure without TMD	0.002986698

Table 12 Maximum relative displacement (m) (Ex.2)

	Records	No TMD		GSA		PSO	
		$U_{\max}$	$U_{\max}$	Reduction (%)	$U_{\max}$	Reduction (%)	
Near-Field Records	Chi-Chi-RSN 1549	0.3752	0.3232	13.84	0.3315	11.64	
	Coyoto Lake-RSN 150	0.2427	0.2358	2.86	0.2357	2.88	
	Kobe-RSN 1120	0.4849	0.3837	20.88	0.4291	11.51	
	Northridge-RSN 1120	3.0632	2.1539	29.69	2.3777	22.38	
	Oroville-RSN 119	1.8050	1.4106	21.85	1.5423	14.55	
Far-Field Records	San Ferando-RSN 63	0.01976	0.01916	3.04	0.01917	3.00	
	Ducze-RSN 1613	0.03893	0.03484	10.52	0.03443	11.57	
	Landers-RSN 3752	0.02609	0.02302	11.74	0.02339	10.34	
	Park Field-RSN 4150	0.05663	0.04085	27.85	0.04583	19.06	

Table 13 Maximum absolute acceleration ( $\text{m/s}^2$ ) (Ex.2)

	Records	No TMD		GSA		PSO	
		$\ddot{U}_{\max}$	$\ddot{U}_{\max}$	Reduction (%)	$\ddot{U}_{\max}$	Reduction (%)	
Near-Field Records	Chi-Chi-RSN 1549	9.1457	8.7472	4.36	8.8047	3.73	
	Coyoto Lake-RSN 150	6.1428	5.9532	3.09	5.9641	2.91	
	Kobe-RSN 1120	5.5962	5.4255	3.05	5.4369	2.85	
	Northridge-RSN 1120	30.1858	21.4143	29.06	23.6344	21.70	
	Oroville-RSN 119	24.9446	21.6373	13.26	22.6999	9.00	
Far-Field Records	San Ferando-RSN 63	0.6075	0.6074	0.01	0.6075	0.00	
	Ducze-RSN 1613	0.5936	0.5529	6.85	0.5540	6.67	
	Landers-RSN 3752	0.7165	0.6278	12.38	0.6449	9.99	
	Park Field-RSN 4150	0.7024	0.5350	23.83	0.5820	17.14	

## 7. Conclusions

The objective of this paper was to propose optimum TMD parameters to reduce the structural responses (RD, AA) as the RD and AA have important roles in the failure of the structure and to decrease the values of the optimum TMD parameters as well. Moreover, optimizing the TMD parameters provides an economical and practical design optimization approach for the buildings. Therefore, two well-known algorithms: GSA and PSO were applied for the optimization goal. To illustrate the performance of these two methods, the responses of two numerical examples of benchmark structures under nine far-field and near-field worldwide earthquakes were investigated.

Results showed that the TMD with the optimum

parameters could reduce the maximum RD and AA in both examples. In the 40-story building example, analyzing the structure under the Tabas earthquake was led to 37% and 36% reduction in RD and 0.31% and 0.38% for AA at the top floor by GSA and PSO algorithms, respectively. Even though the reduction percentage for the RD is approximately 6% more than the reference one in both proposed algorithms, the optimum parameters have been reduced, too. The values of stiffness, damping coefficient and mass reduction percentage are 29.2, 47.7 and 1.9% in the GSA and 23.3, 47.3 and 2.1% with the PSO algorithm compared to the Ant Colony method. The investigation of the building under nine earthquakes showed that the RD has been reduced up to 43.8% by GSA and 50.5% by the PSO and 21% and 25% reduction in AA by the GSA and PSO, respectively. The investigation of story drift demonstrates more relatively uniform distribution. It means that all stories have somehow similar contributions in total building displacement showing an optimum scenario.

Results for the 10-story building example showed that although the maximum RD under the El-Centro earthquake reduced just 1 to 3% for the mean value compared to that of the Genetic Algorithm (GA), the TMD parameters including mass, damping and stiffness ratio reduced by 51, 29 and 26% for the GSA and 63, 19 and 10% for the PSO, respectively. Moreover, the investigation of the responses of the structure under nine earthquakes showed that the RD reduced up to 29.7% by the GSA and 22.4% by the PSO, as well. The reduction percentage for the AA is up to 29.1% by the GSA and 21.7% by the PSO algorithm. The evaluation of the drift also illustrates that TMD has a positive effect on the story drift. The reduction percentage of the story drift is 29.5% by the GSA and 24.1% by the PSO. The optimum TMD parameters acquired by these two methods are smaller than those obtained by the other methods. It results in reduction of acting force from TMD having smaller stiffness and damping factors leading to a cost effective scenario. In addition, results reveal that almost a uniform deformation is obtained using the optimized TMD. This trend reduces the potential of soft story event in the structure during earthquake.

## References

- Adarsh, S. and Janga Reddy, M. (2015), "Gravitational search algorithm for probabilistic design of HBPS canals", *ISH J. Hydraulic Eng.*, **21**(3), 290-297.
- Ahmadi, A., Karray, F. and Kamel, M.S. (2010), "Flocking based approach for data clustering", *Natural Comput.*, **9**(3), 767-791.
- Clough, R.W. and Penzien, J. (1993), *Dynamics of Structures*, McGraw-Hill, New York.
- Daei, M., Sokhangou, F. and Hejazi, M. (2016), *A new intelligent algorithm for damage detection in frames via modal properties*, Taylor and Francis Ltd.
- Desu, N.B., Deb, S.K. and Dutta, A. (2006), "Coupled tuned mass dampers for control of coupled vibrations in asymmetric buildings", *Struct. Control Hlth. Monit.*, **13**(5), 897-916.
- Duman, S., Güvenç, U., Sönmez, Y. and Yörükeren, N. (2012), "Optimal power flow using gravitational search algorithm", *Energy Convers. Manage.*, **59**, 86-95.
- Farshidianfar, A. and Soheili, S. (2013), "Ant colony optimization

- of tuned mass dampers for earthquake oscillations of high-rise structures including soil - structure interaction", *Soil Dyn. Earthq. Eng.*, **51**, 14-22.
- Frahm, H. (1911), Device for damping of bodies, US Patent. NO: 989,958
- Ghashochi-Bargh, H. and Sadr, M. (2013), "PSO algorithm for fundamental frequency optimization of fiber metal laminated panels", *Struct. Eng. Mech.*, **47**(5), 713-727.
- Hadi, M.N.S. and Arfiadi, Y. (1998), "Optimum design of absorber for MDOF structures", *J. Struct. Eng.*, **124**(11), 1272-1280.
- Kaveh, A., Bakhshpoori, T. and Afshari, E. (2015), "Hybrid PSO and SSO algorithm for truss layout and size optimization considering dynamic constraints", *Struct. Eng. Mech.*, **54**(3), 453-474.
- Kaveh, A. and Talatahari, S. (2012), "A hybrid CSS and PSO algorithm for optimal design of structures", *Struct. Eng. Mech.*, **42**(6), 783-797.
- Kennedy, J. and Eberhart, R. (1995), "Particle swarm optimization", *IEEE International Conference on Neural Networks - Conference Proceedings*.
- Kennedy, J., Eberhart, R.C. and Shi, Y. (2001), *Swarm Intelligence*, San Francisco, Morgan Kaufmann Publishers
- Khajehzadeh, M., Taha, M.R., El-Shafie, A. and Eslami, M. (2012), "Optimization of shallow foundation using gravitational search algorithm", **4**(9), 1124-1130.
- Khajehzadeh, M., Taha, M.R. and Eslami, M. (2013), "Efficient gravitational search algorithm for optimum design of retaining walls", **45**(1), 111-127.
- Khatibinia, M. and Sadegh Naseralavi, S. (2014), "Truss optimization on shape and sizing with frequency constraints based on orthogonal multi-gravitational search algorithm", **333**(24), 6349-6369.
- Lee, C.L., Chen, Y.T., Chung, L.L. and Wang, Y.P. (2006), "Optimal design theories and applications of tuned mass dampers", *Eng. Struct.*, **28**(1), 43-53.
- Pourzeynali, S., Lavasani, H.H. and Modarayi, A.H. (2007), "Active control of high rise building structures using fuzzy logic and genetic algorithms", *Eng. Struct.*, **29**(3), 346-357.
- Precup, R.E., David, R.C., Petriu, E.M., Preitl, S. and Radac, M.B. (2012), "Novel adaptive gravitational search algorithm for fuzzy controlled servo systems", *IEEE Trans. Indust. Inform.*, **8**(4), 791-800.
- Ramezani, M., Bathaei, A. and Zahrai, S.M. (2017), "Designing fuzzy systems for optimal parameters of TMDs to reduce seismic response of tall buildings", *Smart Syst. Struct.*, **20**(1), 61-74.
- Randall, S., Halsted, D. and Taylor, D.L. (1981), "Optimum vibration absorbers for linear damped systems", *J. Mech. Des.*, ASME, **103**(4), 908-913.
- Rashedi, E., Nezamabadi-pour, H. and Saryazdi, S. (2009), "GSA: A gravitational search algorithm", *Inform. Sci.*, **179**(13), 2232-2248.
- Rashedi, E., Nezamabadi-Pour, H. and Saryazdi, S. (2011), "Filter modeling using gravitational search algorithm", *Eng. Appl. Artificial Intel.*, **24**(1), 117-122.
- Sabri, N.M., Puteh, M. and Mahmood, M.R. (2013), "A review of gravitational search algorithm", **5**(3), 1-39.
- Sadek, F., Mohraz, B., Taylor, A.W. and Chung, R.M. (1997), "A method of estimating the parameters of tuned mass dampers for seismic applications", *Earthq. Eng. Struct. D.*, **26**(6), 617-635.
- Saravanan, M., Slochanal, S.M.R., Venkatesh, P. and Abraham, J.P.S. (2007), "Application of particle swarm optimization technique for optimal location of FACTS devices considering cost of installation and system loadability", *Electric Pow. Syst. Res.*, **77**(3), 276-283.
- Shariatmadar, H. and Razavi, H.M. (2014), "Seismic control response of structures using an ATMD with fuzzy logic controller and PSO method", *Struct. Eng. Mech.*, **51**(4), 547-564.
- Singh, M.P., Singh, S. and Moreshchi, L.M. (2002), "Tuned mass dampers for response control of torsional buildings", *Earthq. Eng. Struct. D.*, **31**(4), 749-769.
- Thompson, A.G. (1981), "Optimum tuning and damping of a dynamic vibration absorber applied to a force excited and damped primary system", *J. Sound Vib.*, **77**(3), 403-415.
- Tsai, H.C. and Lin, G.C. (1993), "Optimum tuned-mass dampers for minimizing steady-state response of support-excited and damped systems", *Earthq. Eng. Struct. D.*, **22**(11), 957-973.
- Warburton, G.B. (1982), "Optimum absorber parameters for various combinations of response and excitation parameters", *Earthq. Eng. Struct. D.*, **10**(3), 381-401.
- Warburton, G.B. and Ayorinde, E.O. (1980), "Optimum absorber parameters for simple systems", *Earthq. Eng. Struct. D.*, **8**(3), 197-217.
- Yoshida, H., Kawata, K., Fukuyama, Y., Takayama, S. and Nakanishi, Y. (2000), "A particle swarm optimization for reactive power and voltage control considering voltage security assessment", *IEEE Trans. Pow. Syst.*, **15**(4), 1232-1239.

CC